Acta Biomaterialia 14 (2015) 22–32

Contents lists available at ScienceDirect

Acta Biomaterialia

journal homepage: www.elsevier.com/locate/actabiomat

Development of a living membrane comprising a functional human renal proximal tubule cell monolayer on polyethersulfone polymeric membrane

Carolien M.S. Schophuizen [a,b,c,1], Ilaria E. De Napoli [d,1], Jitske Jansen [a,b,c], Sandra Teixeira [d], Martijn J. Wilmer [c], Joost G.J. Hoenderop [b], Lambert P.W. Van den Heuvel [a,e], Rosalinde Masereeuw [c], Dimitrios Stamatialis [d,*]

[a] Department of Pediatric Nephrology, Radboudumc, Nijmegen, The Netherlands
[b] Department of Physiology, Radboudumc, Radboud Institute for Molecular Life Sciences, Nijmegen, The Netherlands
[c] Department of Pharmacology and Toxicology, Radboudumc, Radboud Institute for Molecular Life Sciences, Nijmegen, The Netherlands
[d] Department of Biomaterials Science and Technology, MIRA Institute for Biomedical Technology and Technical Medicine, University of Twente, Enschede, The Netherlands
[e] Department of Pediatrics, Catholic University Leuven, Leuven, Belgium

ARTICLE INFO

Article history:
Received 23 June 2014
Received in revised form 22 November 2014
Accepted 2 December 2014
Available online 17 December 2014

Keywords:
Renal assist device
Living membrane
Human kidney proximal tubule cells
Membrane biofunctionalization
L-DOPA

ABSTRACT

The need for improved renal replacement therapies has stimulated innovative research for the development of a cell-based renal assist device. A key requirement for such a device is the formation of a "living membrane", consisting of a tight kidney cell monolayer with preserved functional organic ion transporters on a suitable artificial membrane surface. In this work, we applied a unique conditionally immortalized proximal tubule epithelial cell (ciPTEC) line with an optimized coating strategy on polyethersulfone (PES) membranes to develop a living membrane with a functional proximal tubule epithelial cell layer. PES membranes were coated with combinations of 3,4-dihydroxy-L-phenylalanine and human collagen IV (Coll IV). The optimal coating time and concentrations were determined to achieve retention of vital blood components while preserving high water transport and optimal ciPTEC adhesion. The ciPTEC monolayers obtained were examined through immunocytochemistry to detect zona occludens 1 tight junction proteins. Reproducible monolayers were formed when using a combination of 2 mg ml^{-1} 3,4-dihydroxy-L-phenylalanine (4 min coating, 1 h dissolution) and 25 μg ml^{-1} Coll IV (4 min coating). The successful transport of ^{14}C-creatinine through the developed living membrane system was used as an indication for organic cation transporter functionality. The addition of metformin or cimetidine significantly reduced the creatinine transepithelial flux, indicating active creatinine uptake in ciPTECs, most likely mediated by the organic cation transporter, OCT2 (SLC22A2). In conclusion, this study shows the successful development of a living membrane consisting of a reproducible ciPTEC monolayer on PES membranes, an important step towards the development of a bioartificial kidney.

1. Introduction

The number of patients with end-stage renal disease (ESRD) is progressively increasing and the need for renal replacement therapies is rising [1]. Worldwide, over 2 million patients suffer from ESRD, and each year that number grows by 5%. Since transplant options are limited [2], ~70% of patients receive (hemodialysis or peritoneal) dialysis treatment. While dialysis therapy has already prolonged many ESRD patients' lives, the treatment cannot completely replace renal function. Mortality (15–20% per year) and morbidity of these patients remain high, whereas their quality of life is generally low. Hemodialysis (HD) therapy removes mainly small, unbound substances from the circulation, while leaving large, compartmentalized and protein-bound uremic retention solutes untouched [3]. Although the introduction of high-flux (HF) or hemodiafiltration (HDF) therapy promotes enhanced removal of middle molecular weight solutes, the removal of protein-bound retention solutes remains limited [4,5].

Since renal secretion of such protein-bound compounds is predominantly mediated by the proximal tubule epithelial cells (PTEC)

* Corresponding author. Tel.: +31 53 4894675.
E-mail address: d.stamatialis@utwente.nl (D. Stamatialis).
[1] Both authors contributed equally.

http://dx.doi.org/10.1016/j.actbio.2014.12.002
1742-7061/

[6,7], the need for improved renal replacement therapy has stimulated innovative research into the development of renal assist devices (RADs) [8]. These innovative devices aim to complement the hemodialysis treatment, by coupling artificial membranes with functional kidney cells. To achieve efficient clearance of uremic retention solutes, proximal tubular epithelial cells need to be seeded on the inner surface of hollow fiber membranes. This situation is comparable to the native tubule, where the basement membrane separates proximal tubule cells from the circulation. While the patients' blood flows over the outer surface, the uremic retention solutes can bind to the transport proteins present on the basolateral surface of human PTEC, facilitating their subsequent secretion into the hemodialysis filtrate. This approach could provide a means to further diminish the systemic accumulation of uremic retention solutes, reduce the incidence of secondary morbidities in patients and shorten dialysis duration or frequency, thereby improving the quality of life in ESRD.

The development of a RAD brings along very specific biotechnological challenges, as was recently reviewed by Jansen et al. [9]. First of all, an important challenge in the development of a RAD is the limited availability of reliable and well-characterized human proximal tubule cells capable of transepithelial excretion of uremic retention solutes. This "living membrane" should consist of tight cellular monolayers maintaining their typical polarity and functionality. Second, one side of the membrane to be used in a RAD needs to be suitable for blood contact (low cell adhesion), whilst the other side should facilitate cellular adhesion. Surface topography was identified as an important feature affecting cell adhesion and membrane hemocompatibility, the two properties being favored by higher surface roughness and smoothness, respectively [10]. Several studies which attempted to create living membranes with renal epithelial cells have used existing membranes (mostly hollow fibers) used in dialysis and/or blood purification. Polyethersulfone (PES), polysulfone (PSF), polyacrylonitrile (PAN) and cellulose acetate membranes were evaluated for their ability to support monolayer growth of renal epithelial cells [11–13]. Since these membranes are designed for low cell adhesion, and maximum hemocompatibility during blood filtration, it is necessary to apply a coating consisting of extracellular matrix components. This actually describes the third challenge in RAD development: the optimization of coating conditions. In some cases, coatings have been reported to improve the attachment of renal tubule epithelial cells, but often coatings failed to maintain trans-monolayer transport activity and monolayer integrity [14–18]. Human collagen type IV (Coll IV) based coatings are promising for the attachment and functional culture of proximal tubule cells [15], since Coll IV is endogenously present in the basal lamina and promotes mesenchymal cell differentiation towards the epithelial lineage [19]. However, it is necessary to improve its adhesion to the artificial membrane. The treatment of polymeric surfaces with biomolecules via covalent reactions is generally inconvenient given the susceptibility of different activated groups to hydrolysis, which can lead to low efficiency of surface biofunctionalization [20]. An easy two-step water-based biofunctionalization method has been proposed that promotes the formation of a thin adherent polydopamine (PDA) film [10,17,21] using self-polymerizing 3,4-dihydroxy-L-phenylalanine (L-DOPA) and exploits the reactivity of the PDA film to covalently bind the biomolecule Coll IV on the membrane surface [10,20]. However, in these earlier studies, the application of the coatings was not optimized with regard to membrane transport characteristics (high water permeance and retention of vital proteins such as bovine serum albumin (BSA) and immunoglobulin G (IgG)).

The selection of renal cell lines suitable for RAD application poses another challenge. The use of animal cell models, such as porcine (primary or LLC-PK1), monkey (JTC-12) and canine (MDCK) renal epithelial cells provides insight into the functionality of a RAD, both in vitro as well as in vivo [13,16,22–25]. However, their clinical application is highly restricted. Moreover, species differences in renal proximal tubule physiology are in favor of a renal cell line of human origin [26,27]. Studies using freshly isolated primary human proximal tubule cells in a RAD have shown promising results [10,28,29]. However, their limited availability, low proliferative capacity and donor-to-donor variation severely restrict the use of these cells. The utilization of a functional human proximal tubule epithelial cell line overcomes these drawbacks. Previously, some of the co-authors of this study developed a human conditionally immortalized proximal tubule epithelial cell (ciPTEC) line, with intact proximal tubular characteristics and endogenous expression of various functional transport proteins [30,31]. Among the advantages of this cell line is the switch between a proliferative state at 33 °C to a differentiation state at 37 °C, permitted by transduction with the temperature-sensitive Simian virus 40 (SV40) large T antigen. The genetic switch allows for cell proliferation arrest when the cells are confluent and fully differentiated, promoting the formation of tight and functional monolayers [32].

In this work, we show for the first time the development of a stable, functional living membrane by culturing ciPTECs on PES-based membranes with a molecular weight cut off of 50 kDa. This cut off prevents albumin leakage, blocks possible immunoglobulin transfer and avoids the loss of vital blood component in the case of cell monolayer integrity failure. The membranes were coated with a double coating consisting of L-DOPA and Coll IV on the more porous rough membrane side to maximize the beneficial effect of both membrane topography and coating on cell adhesion. This coating was carefully optimized to preserve high membrane permeability and create a tight cell monolayer. The selective active transport of creatinine through the living membranes was investigated in the presence and absence of specific inhibitors, and compared to a commercially available polyester Transwell® system.

2. Materials and methods

2.1. Membrane coatings

Flat polyethersulfone membranes (Sartorius, Goettingen, Germany), which showed good hemocompatibility properties [33], with a molecular weight cut off of 50 kDa (indicated, as PES-50) were coated with a double layer of L-DOPA (D9628, Sigma Aldrich, Zwijndrecht, The Netherlands) and human Coll IV (C6745, Sigma Aldrich, Zwijndrecht, The Netherlands) L-DOPA solutions with concentrations ranging from 1 to 2 mg ml^{-1} in Tris buffer 10 mM (pH 8.5) were prepared and dissolved at 37 °C. Complete dissolution was obtained after 1 h, followed by filter sterilization. Subsequently, the L-DOPA solution was either used to coat the membranes immediately after powder dissolution, with minimum polymerization degree (referred to as L-DOPA (1 h)), or left to polymerize for an additional 2 h (referred to as L-DOPA (3 h)) before coating the membranes. For the sake of simplicity, we defined the dissolution time as the time that the L-DOPA is kept in solution before coating the membrane. The membranes were first pre-incubated in Hanks' balanced salt solution (HBSS; Life Technologies, Bleiswijk, The Netherlands) for 10 min. Next, the L-DOPA solutions were applied to the membrane surface. The solution was aspirated, and the membranes were left to dry for 5 min. A Coll IV solution (25 μg ml^{-1} or 50 μg ml^{-1}) in HBSS was then used for the second step of the coating. After fluid aspiration and drying, the membranes were washed three times in HBSS to remove any remaining solvent or unbound compound. Diverse L-DOPA dissolution times (1 and 3 h) and coating times of membranes (1 and 4 min) were tested and their effects on membrane properties were evaluated

in terms of membrane morphology and pure water permeance. An overview of the coating conditions tested is given in Fig. 1. The PES-50 membrane has an asymmetric structure: one membrane side is denser (and therefore determines the transport properties) and smooth, while the other membrane side is more porous and rough. The double coating was performed on the more porous membrane side, under static conditions, by contacting the coating solution with the membrane surface. To obtain a single sided-coating of the flat PES membranes, the coating solution was first poured into glass Petri dishes and the membrane was gently placed on the top of the solutions with the porous side in contact with the liquid. The selection of final concentrations, dissolution times and coating times for both the L-DOPA and the Coll IV solution was based on cell adhesion, cell monolayer formation and tight junction expression. Reproducibility of the coating was investigated in terms of water and protein transport properties. For cell culturing, Corning (Corning Costar, NY, USA) custom Transwell® supports were used. In these Transwells (12 mm in diameter), the polyester cell membrane was replaced by PES-50 membrane used for the double coating development. Here, membrane coating was performed on one side of the membrane by applying the solutions to the apical (cell-facing) side of the Transwell®. Since the PES membrane is sealed on the perimeter to the plastic holder, the basolateral side of the membrane did not come into direct contact with the coating solution. Fig. A.1 in the appendix provides a schematic overview of a coated Transwell® membrane. As a reference, we employed double-coated (positive control) polyester Transwell® membranes, which are frequently used for in vitro PTEC culture [30,34].

2.2. Membrane morphological and surface composition analysis

Membrane morphology was determined by scanning electron microscopy (SEM; FEI/Philips XL30 FEG ESEM). Surface samples were prepared and kept overnight at 30 °C and gold-sputtered before examination by SEM at a voltage of 5 kV. The membrane surface chemical structures and composition of the coated and uncoated PES-50 were characterized using attenuated total reflection Fourier transform infrared spectra (ATR-FTIR) (Spectrum two, Perkin Elmer, Waltham, USA) instrument. Elementary analysis of the membrane composition was performed by energy-dispersive spectroscopy analysis (EDS; EDAX; Apollo X for ESEM, NJ, USA).

2.3. Membrane transport properties

Pure water, BSA (A2153, Sigma Aldrich, Zwijndrecht, The Netherlands) and IgG (I9640, Sigma Aldrich, Zwijndrecht, The Netherlands) solution permeance was determined using an air-pressurized dead-end "Amicon type" ultrafiltration cell (hosting 4 cm diameter membrane samples) and ultrapure water. The flux (J) of water and protein solution through the membranes at each pressure was determined by collecting the mass of the permeated liquid over time and correlating it to the membrane unit surface area. The permeance (L, in $l\,h^{-1}\,m^{-2}\,bar^{-1}$) of water or protein solution was estimated by normalizing the water or protein solution flux (J, in $l\,h^{-1}\,m^{-2}$) by the applied transmembrane pressure (ΔP, in bar). The permeance is, in fact, calculated from the slope of the linear part of the flux vs. transmembrane pressure relationship:

$$L = \frac{J}{\Delta P} \tag{1}$$

Clean water permeation tests were performed by using ultrapure water (MilliQ 18 MΩ cm, Millipore; Billerica, MA, USA) solutions inside stirred amicon cells (Millipore; Billerica, MA, USA), where the membranes were placed with the thin layer facing the feed solution. Automatic collection of permeate mass during time was performed by means of a Labview based software; the mass was converted to volume given the water density equal to 998 kg m^{-3} at 20 °C [35]. Uncoated flat membranes were tested

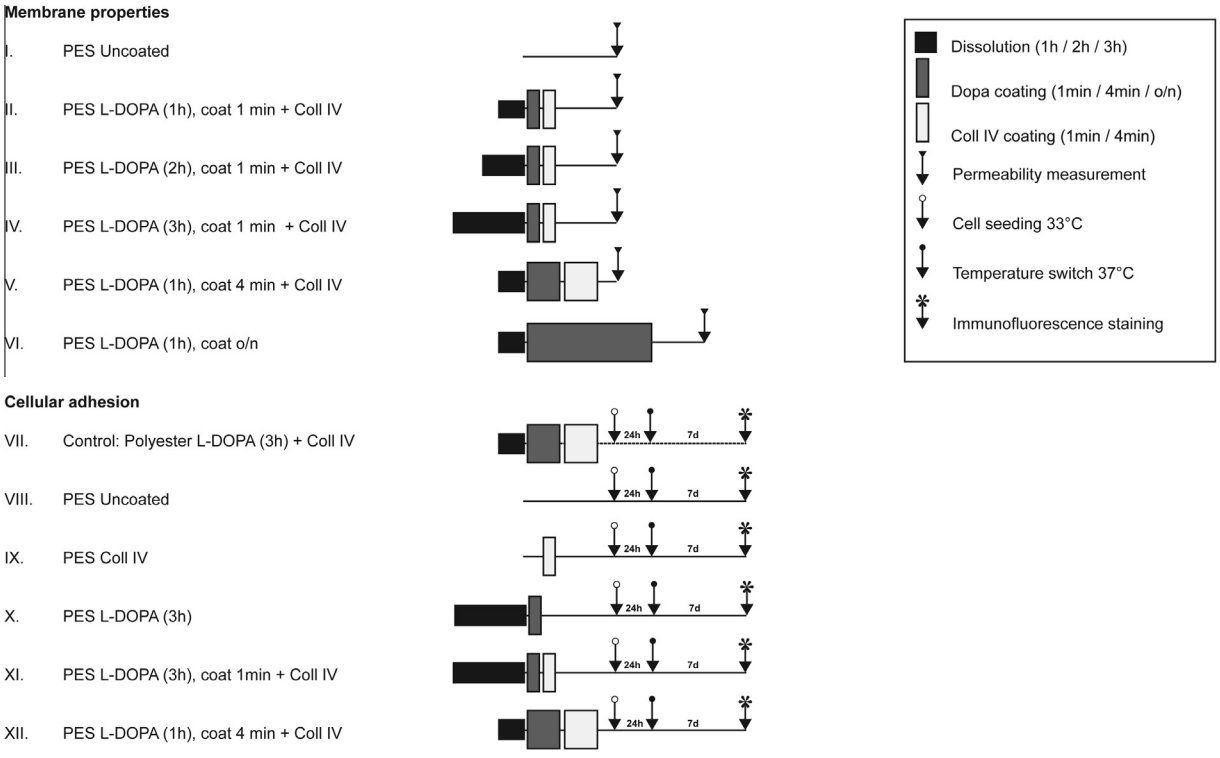

Fig. 1. Schematic overview of the coating conditions evaluated for their membrane properties and cell adhesion. See text for further details and abbreviations.

after immersing them in pure water for 1 h to remove preservatives added during the manufacturing process. Membranes double-coated with L-DOPA and Coll IV were immersed in HBSS buffer for 30 min before they were used. Subsequently, the membranes were subject to a flushing step with ultrapure water at the highest working pressure (0.75 bar). Then, down-to-up pressure cycles were applied to each membrane.

The extent of protein transport through the membrane was evaluated by estimating the apparent sieving coefficient (SC_a):

$$SC_a = \frac{C_p}{C_b} \quad (2)$$

where C_p is the protein concentration in the permeate and C_b is the protein concentration in the feed protein solution. $SC_a = 1$ means that the protein passes freely through the membrane, while $SC_a = 0$ means that the membrane rejects the protein completely.

Phosphate buffered saline (PBS) containing BSA or IgG was used at a concentration of 1 mg ml^{-1} and 0.02 mg ml^{-1}, respectively. Three different pressures (0.25, 0.50, 0.75 bar) were applied and sample collection occurred every 15 min for 1 h. The protein solution was continuously mixed at the top of the membrane surface to prevent polarization concentration effect and delay membrane fouling. BSA and IgG concentration was evaluated by spectrophotometric analysis in quartz cuvettes at 280 nm.

2.4. Cell culture

A previously developed ciPTEC cell line [30] was used for functional testing of the coated membranes. In short, this immortal cell line was developed by transducing primary human proximal tubule epithelial cells, obtained from urine samples of healthy volunteers, with a SV40t, and hTERT gene. SV40t stimulates cellular proliferation at 33 °C, while it is silenced by culturing the cells in a 37 °C environment. As a consequence, at 37 °C the cells are able to differentiate and form a tight monolayer. The hTERT ensures the cellular quality, by keeping the length of the telomeres intact during proliferation. We have previously evaluated the characteristics of this cell line, on a morphological and functional level [7,31]. CiPTECs were cultured in Dulbecco's modified Eagle medium DMEM-HAM's F12 (Lonza; Basel, Switzerland) containing 10% v/v fetal calf serum (FCS; Greiner Bio-One; Alphen a/d Rijn, The Netherlands), 5 μg ml^{-1} insulin, 5 μg ml^{-1} transferrin, 5 ng ml^{-1} selenium, 36 ng ml^{-1} hydrocortisone, 10 ng ml^{-1} epidermal growth factor and 40 pg ml^{-1} tri-iodothyronine, all purchased from Sigma–Aldrich Co. (Zwijndrecht, The Netherlands). Culture media were phenol-red and antibiotic free. To prevent de-differentiation of ciPTECs during regular culturing, cells were used in experiments up to a maximum of 40 passages, during which proximal tubular characteristics remained unaltered [30]. Proliferating ciPTEC were seeded onto the polyester or PES membrane Transwell® inserts at a density of 133.000 cells cm^{-2}. To promote initial cellular attachment and proliferation, ciPTECs were cultured for 24 h at 33 °C 5% (v/v) CO_2 and after this time period the temperature was changed to 37 °C for 7 days to promote the formation of a differentiated monolayer.

2.5. Immunocytochemistry

To investigate morphological characteristics and monolayer integrity of matured ciPTECs cultured on polyester [30,34] and PES-50 Transwell® inserts, immunocytochemistry was performed, and after 7 days the expression of the tight junction protein, zonula occludens 1 (ZO-1) was studied. Matured ciPTECs were fixed using 2% (w/v) paraformaldehyde in HBSS supplemented with 2% (w/v) sucrose for 5 min and permeabilized in 0.3% (v/v) Triton X-100 in HBSS for 10 min. To prevent non-specific binding of antibodies, cells were exposed to a block solution containing 2% (w/v) BSA fraction V (Roche, Woerden, The Netherlands) and 0.1% (v/v) Tween-20 in HBSS for 30 min. Cells were incubated with antibodies diluted in block solution against the tight junction protein ZO-1 (1:50 dilution, Invitrogen, Carlsbad, CA) for 1 h, followed by incubation with goat-anti-rabbit-Alexa488 conjugate (1:200, Life Technologies Europe BV, Bleiswijk, The Netherlands) for 30 min. Finally, DAPI nuclei staining (300 nM, Life Technologies Europe BV) was performed for 5 min. Protein expression and localization were examined using the Olympus FV1000 confocal laser scanning microscope (Olympus, Tokyo, Japan) and images were captured using the Olympus software FV10-ASW version 1.7. To semi-quantify the fluorescent staining of ZO-1, a grid of 8.5 μm^2 was placed on top of the confocal images using ImageJ software (ImageJ 1.46r, NIH, USA) [36]. The number of intersections between the grid and the ZO-1 signal was determined for each condition.

2.6. Transepithelial transport measurements

Transepithelial transport of [^{14}C]creatinine by matured ciPTEC monolayers cultured on either polyester or PES Transwell® inserts was measured using a Transwell® culture system. A schematic overview of the set-up is provided in the appendix (Fig. A.1). Polyester Transwells® (diameter 12 mm, pore size 0.4 μm) were coated with L-DOPA alone or in combination with Coll IV (25 mg ml^{-1}, for 2 h), and compared to double-coated polyester or PES-50 Transwells®. Mature cell monolayers were washed in modified Krebs–Henseleit buffer (Sigma–Aldrich, Zwijndrecht, The Netherlands) including 10 mM Hepes (pH 7.4). Subsequently, all membranes tested were pre-incubated for 2 h at 37 °C, 5% (v/v) CO_2 in Krebs–Henseleit–Hepes buffer (0.5 ml apically, 1.5 ml basolaterally). Transport was initiated by the basolateral addition of either [^{14}C]creatinine (0.75 μM, 2 μCi ml^{-1}) or [^{3}H]inulin (0.45 μM, 20 μCi ml^{-1}) with or without cimetidine (100 μM) or metformin (100 μM) as competitors for the transport of organic cation transporter OCT2 (Sigma–Aldrich Co., Zwijndrecht, The Netherlands). At the start of the measurement, a 20 μl reference sample was taken from the basolateral exposure compartment. After 30 min of incubation with gentle agitation at 37 °C a 200 μl sample was removed from the apical chamber. The activity of [^{3}H] and [^{14}C] in the samples was determined by liquid scintillation counting (Beckman). Fluxes of [^{14}C]creatinine or [^{3}H]inulin were determined for each separate Transwell®. The flux of [^{3}H]inulin was used as an internal leakage marker. The basolateral to apical flux (J) was calculated with:

$$J = \frac{dQ}{S * dt} \quad (3)$$

where dQ = amount transported (pmol); dt = duration of transport (min); S = surface area (cm^2).

2.7. Data analysis

Water, BSA and IgG transport measurements in each experiment were performed at least in triplicates ($N \geqslant 3$ for each coating condition). Results are presented as mean ± standard deviation. Statistical analysis was performed with the Microsoft Excel® software (Microsoft Corporation, Seattle, USA) using a one-way analysis of variance (ANOVA) or Student's t-test when appropriate.

Quantification of ZO-1 staining on Transwell® polyester or PES membranes was performed in triplicate for each coating condition. The results are presented as mean ± standard error of the mean. Results were normalized by taking the double-coated polyester Transwell® as 100% reference. One-way ANOVA followed by a Dunnett's post test was performed using GraphPad Prism version 6.00 for Windows (GraphPad Software, La Jolla, CA, USA).

For basolateral creatinine transport experiments in the commercially available polyester Transwells® the experiments were performed at least in triplicate in three independent experiments. The custom PES Transwells® were tested in duplicate in three independent experiments. Results are presented as mean ± standard error of the mean. Statistical analysis was performed with GraphPad Prism, using a two-way ANOVA combined with Bonferroni's post test.

3. Results and discussion

The biofunctionalization strategy of flat PES-50 membranes was optimized first to develop functional ciPTEC monolayers. Artificial membranes should provide a solid base for cells to form tight monolayers and facilitate active transepithelial solute transport. In the nephron, the proximal tubule is responsible for the reabsorption of 65% of all the water filtered by the glomerulus; the very high permeability of the tissue was estimated to be $\sim 1 \times 10^5$ l m^{-2} h^{-1} bar^{-1} [37]. The hydraulic permeability of native PES-50 membrane is two orders of magnitude lower than the value reported for natural tissue; the membrane was chosen on the base of its capacity to retain vital blood components, consistent with other research in the field [22]. For this reason, water transport through the coated membranes was one of the main parameters to optimize, in order to preserve the highest permeance possible.

A recent study proposed the application of an overnight double coating [10]. However, when we applied such a coating, a significant decrease in membrane water permeance (39 ± 23 l m^{-2} h^{-1} bar^{-1}) was detected in comparison to uncoated membranes (738 ± 110 l m^{-2} h^{-1} bar^{-1}). Further reduction of the permeance was expected when applying the second coating layer consisting of Coll IV. To avoid significant transport limitations, we investigated shorter L-DOPA dissolution times. In a first attempt, L-DOPA was used for the coating immediately after the dissolution step (L-DOPA (1 h)). The average value of water permeance did not change significantly (654 ± 70 l m^{-2} h^{-1} bar^{-1}) with respect to uncoated membrane values (Fig. 1, I). After applying the Coll IV coating on top of the L-DOPA layer (Fig. 1, II), the average value of water permeance decreased to 347 ± 151 l m^{-2} h^{-1} bar^{-1}. However, the high coefficient of variation (0.44) indicated a non-reproducible coating. These results indicate that short coating times do not cause significant changes, whilst overnight coating results in a dramatic reduction in membrane transport properties. Since the variable "time" plays a central role in the macroscopic transport properties of the coated membrane, we compared the effects of prolongation of the L-DOPA dissolution time (Fig. 1; II, III and IV), to prolongation of the coating time to L-DOPA and Coll IV from 1 to 4 min (Fig. 1; II and V).

When applying L-DOPA coating alone, prolongation of the L-DOPA dissolution time slightly increases the average membrane water permeance, although this effect was not significantly different from the non-coated PES-50 membranes (dark symbols, Fig. 2a). Literature reports that L-DOPA coating can increase the membrane hydrophilicity due to the coexistence of carboxylic and amino groups in the L-DOPA molecule [38]. In fact, the effect of L-DOPA coating on hydrophilization of different materials has been shown by the reduction of water contact angle under the same experimental conditions used in the present study (pH, Tris buffer molarity and L-DOPA concentration) [21,38,39]; we therefore expect that our membranes are slightly hydrophilized, too. Nevertheless, the application of L-DOPA to porous membranes can reduce the membrane transport properties. This decrease mostly occurs to UF membranes where the pore dimensions allow the migration of L-DOPA monomers and oligomers inside the membrane structure with s consequent reduction or blockage of the inner porosity [40,41]. The transport properties of reverse osmosis (RO) and microfiltration (MF) membranes were reported to be less affected by L-DOPA coatings, due to the different pore size [41]. Since we used PES-50 UF membranes, the coating time as well as the L-DOPA dissolution time required optimization to avoid complete suppression of the membrane permeance.

The Coll IV coating on top of the L-DOPA layer (Fig. 1, conditions I–IV) decreased the membrane water permeance significantly (open symbols in Fig. 2a). The permeance for the double-coated membranes with L-DOPA (3 h) and Coll IV for 1 min was 194 ± 35 l m^{-2} h^{-1} bar^{-1}, which is significantly lower than the uncoated membranes. However, when compared to overnight L-DOPA coating (Fig. 1, VI), the membrane permeance improved markedly. Furthermore, prolongation of L-DOPA dissolution to 3 h enhanced the coating reproducibility, as demonstrated by the low standard deviation of the permeance values. Fig. 2b presents the optimization procedure of the double coating using different coating times of L-DOPA (1 h) (Fig. 1; II, V and VI). The water permeance for double-coated membranes with 4 min coating was 2.7-fold higher (146 ± 10 l m^{-2} h^{-1} bar^{-1}) than for overnight L-DOPA (only) coating. Prolongation of coating time to 4 min also improved the double coating reproducibility, as demonstrated by the low standard deviation of the permeance results. These results

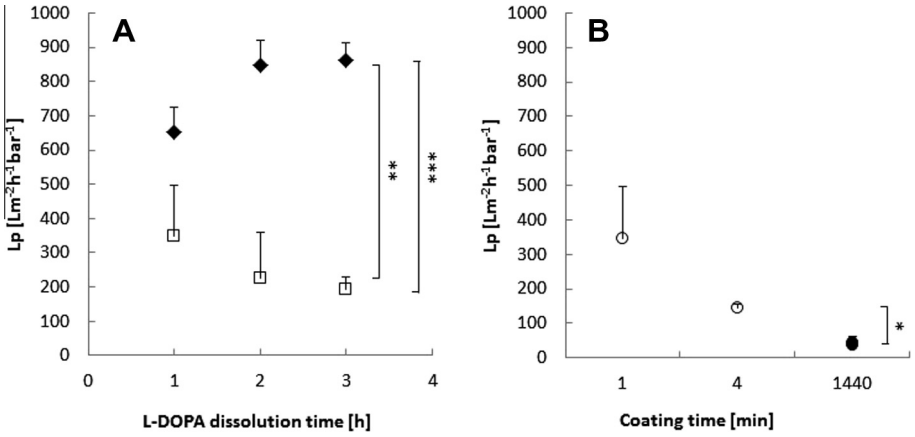

Fig. 2. Pure water permeance of PES-50 membranes coated with L-DOPA (2 mg ml^{-1}) and Coll IV (25 μg ml^{-1}) as a function of: (a) L-DOPA dissolution time for PES membranes coated for 1 min with L-DOPA solution only (♦), or L-DOPA followed by Coll IV (□); (b) double coating with L-DOPA followed by Coll IV with varying coating times (○), or L-DOPA solution after overnight coating (●). Data are presented as mean ± standard error, $^{*}p < 0.05$; $^{**}p < 0.01$; $^{***}p < 0.005$; $N \geqslant 3$ for each experimental point.

indicate that optimization of the L-DOPA dissolution and coating times significantly improves the membrane permeance and coating reproducibility, when compared to overnight coating.

The progressive reduction of membrane water permeance correlated with the observed morphological changes at the porous side of the membrane surface where the double coating was applied. Fig. 3 presents SEM images of uncoated, only L-DOPA and double-coated membrane surfaces. The single L-DOPA coating slightly affected the porous layer morphology (data not shown). After application of L-DOPA (3 h), an estimated 40% reduction in the macroporosity visible at the upper surface of the flat membranes could be observed compared with the original membranes (Fig. 3b). Application of Coll IV to the L-DOPA coating resulted in complete occlusion of membrane surface pores as compared to membranes coated with L-DOPA only, for all L-DOPA dissolution times tested (Fig. 3c). The lack of visible differences in surface morphology in the presence of the single L-DOPA coating in comparison with native membranes was consistent with the average rate of PDA layer deposition (2 nm h^{-1}) reported in previous studies for the same experimental conditions (L-DOPA concentration, temperature, pH and tris buffer molarity) [21,42]. The analysis of membrane surface chemical composition confirmed

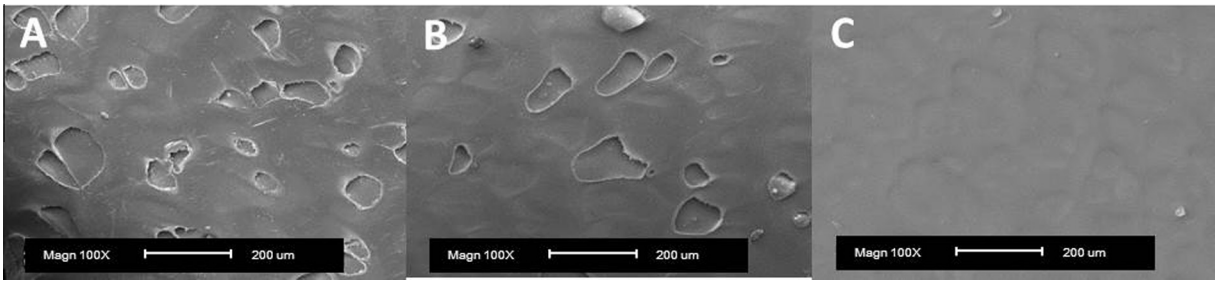

Fig. 3. Representative SEM analysis of PES-50 membranes porous side surface morphology with L-DOPA (2 mg ml^{-1}) and Coll IV (25 μg ml^{-1}) with different L-DOPA dissolution times: (a) uncoated; (b) 1 min coating with L-DOPA (3 h) only; (c) 4 min coating with L-DOPA (1 h) and Coll IV. Magnification 100×. At least three independent membranes were examined for each condition.

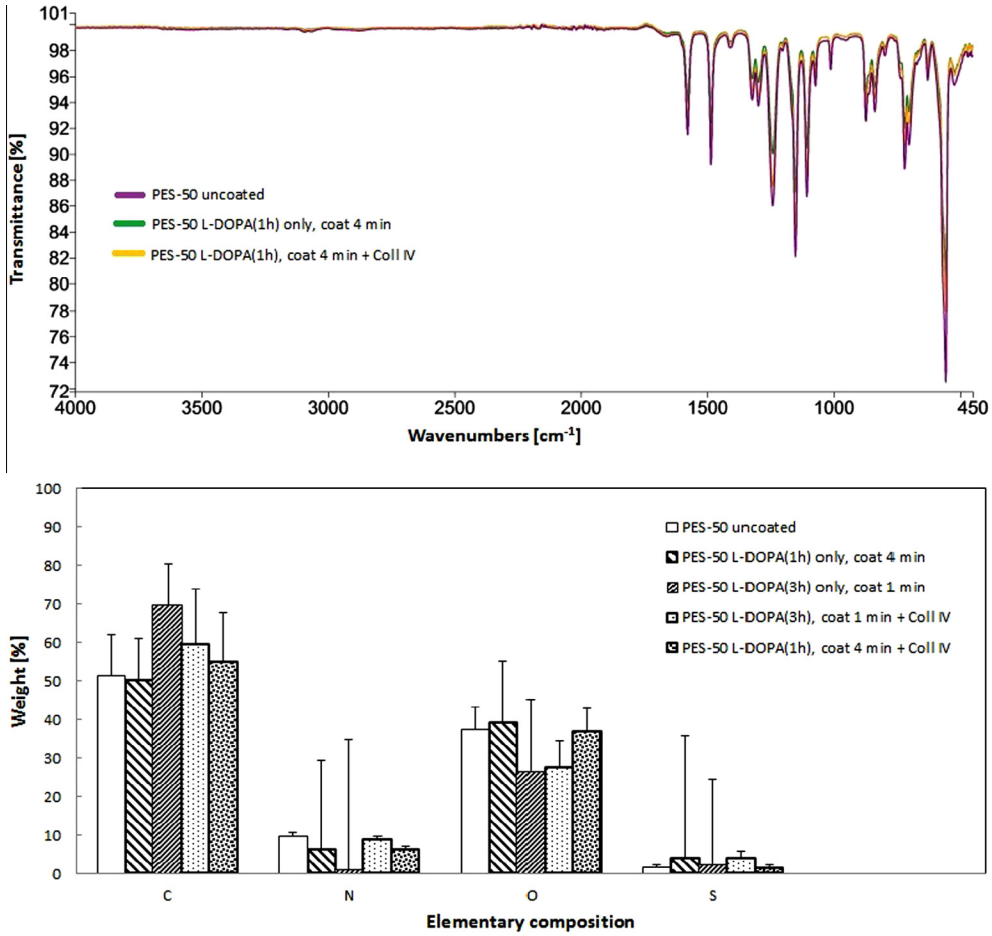

Fig. 4. Surface chemical composition of PES-50 membranes uncoated and coated with L-DOPA (2 mg ml^{-1}) and Coll IV (25 μg ml^{-1}). Top: ATR-FTIR spectra for: (purple) uncoated PES-50; (green) 4 min coating with L-DOPA (1 h) only; (yellow) 4 min coating with L-DOPA (1 h) and Coll IV. Bottom: EDS analysis of (from left to right: uncoated PES-50; 4 min coating with L-DOPA (1 h) only; 1 min coating with L-DOPA (3 h) only; 1 min coating with L-DOPA (3 h) and Coll IV; 4 min coating with L-DOPA (1 h) and Coll IV.

that the thickness of the coating was in the nm range, as the beam penetration for both EDS and Fourier transform infrared (FTIR) analysis was deeper than the single or double coating applied. In fact, for both the FTIR spectrum and the elementary composition, the underlying PES material is still dominant (Fig. 4). Dopamine monomers and small oligomers have previously been demonstrated to play a primary role in the initiation of the PDA deposition and its consequent polymerization at the membrane surface [21,41,42]. In these studies, maximal monomer deposition rate was observed during the first hours after L-DOPA dissolution. This finding may explain why, in our case, a short coating time was sufficient to modify the PES-50 membranes, providing good collagen IV adhesion and reproducibility of transport properties.

The optimized coatings were tested further for optimal cell monolayer formation by ZO-1 tight junction protein expression, a marker that indicates monolayer integrity and polarity of epithelial cells. The tested coating conditions are described schematically in Fig. 1, under the cellular adhesion heading (Fig. 1; conditions VII–XII). Standard double-coated polyester Transwell® inserts were used as a positive control (Fig. 5a). Uncoated PES-50 membranes provided poor cell adhesion of ciPTEC (Fig. 5b) while single coating with Coll IV (25 mg ml^{-1}) or L-DOPA (2 mg ml^{-1}) did not improve this (Fig. 5c and d). After application of the double coating, cellular adhesion and the expression of ZO-1 improved (Fig. 5e and f). The observed clear ZO-1 expression indicates polarization of the monolayer, improving epithelial characteristics [43], and limits paracellular leakage. No significant difference in monolayer formation and ZO-1 expression was detected between conditions XI and XII (Fig. 5e and f), which varied either the coating or dissolution time. Furthermore, quantification of the ZO-1 has indicated that ciPTEC expressed ZO-1 protein in a similar fashion on both double-coated PES-50 as on polyester Transwells®, which are considered the golden standard in ciPTEC transepithelial studies (Fig. 5g). Lowering the concentration of L-DOPA reduced the reproducibility of cellular adhesion, even in the presence of a higher Coll IV concentration, thus suggesting the importance of a good L-DOPA layer to foster Coll IV membrane coating. Furthermore, increasing the Coll IV concentration to 50 μg ml^{-1} after 2 mg ml^{-1} L-DOPA coating did not improve monolayer quality with respect to 25 μg ml^{-1} Coll IV (Fig. A.2 in the appendix).

The coatings were investigated further in terms of protein rejection and fouling phenomena during protein solution permeance. Table 1 shows a comparison of transport properties of uncoated and membranes with optimized coatings (Fig. 1; conditions I, IV and V). The permeance of IgG and BSA solutions for the uncoated PES-50 membranes is 53 ± 11 and 57 ± 7 l m^{-2} h^{-1} bar^{-1}, respec-

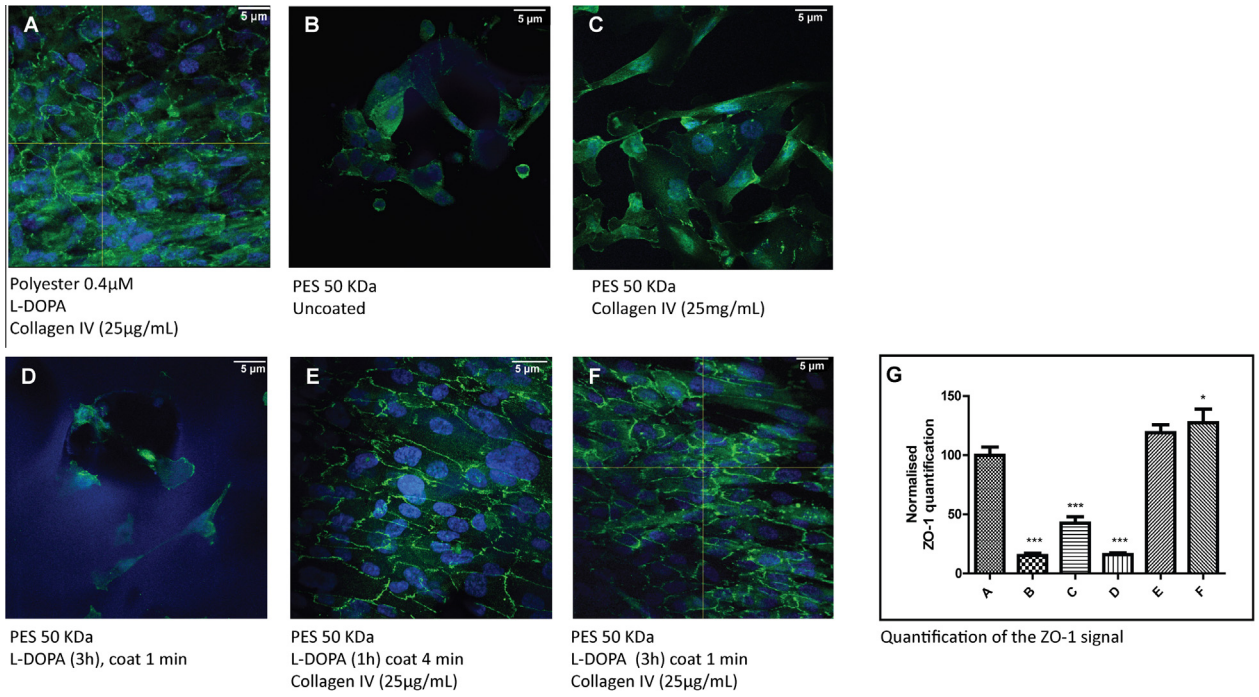

Fig. 5. Representative images of immunocytochemical analysis of the ZO-1 tight junction protein (green) and nuclei (blue) in ciPTEC monolayers cultured on membranes with varying coating times: (a) L-DOPA (2 mg ml^{-1}) and Coll IV (25 μg ml^{-1}) double-coated polyester Transwell® inserts; (b) uncoated PES-50 Transwell® insert; (c) Coll IV (25 μg ml^{-1}) coated PES-50 Transwell® inserts (d) L-DOPA (2 mg ml^{-1}) coated PES-50 insert; (e) PES-50 Transwell® inserts coated for 4 min with L-DOPA (1 h) and Coll IV; (f) PES-50 Transwell® inserts coated for 1 min with L-DOPA (3 h) and Coll IV; (g) ZO-1 abundance in ciPTEC monolayers compared to double-coated polyester Transwell® inserts. At least three independent membranes were examined for each condition. $^{***}p < 0.005$. Magnification 60×.

Table 1
Comparison of the transport properties of uncoated PES-50 membrane and coated with L-DOPA (2 mg ml^{-1}) and Coll IV (25 μg ml^{-1}) with two approaches: (1) 1 min coating with L-DOPA (3 h) and 1 min Coll IV; and (2) 4 min coating with L-DOPA (1 h) and 4 min Coll IV.

		Uncoated		1 min L-DOPA (3 h) + 1 min coll IV		4 min L-DOPA (1 h) + 4 min coll IV	
Pure water permeance	[L m^{-2} h^{-1} bar^{-1}]	738	±110	194	±35	146	±10
BSA solution permeance	[L m^{-2} h^{-1} bar^{-1}]	57	±7	44	±8	37	±27
IgG solution permeance	[L m^{-2} h^{-1} bar^{-1}]	53	±11	65	±24	51	±12
BSA $SC_a = C_P/C_b$	[–]	0,03	±0,01	0,06	±0,02	0,02	±0,01
IgG $SC_a = C_P/C_b$	[–]	0,02	±0,01	0,05	±0,03	0,04	±0,03

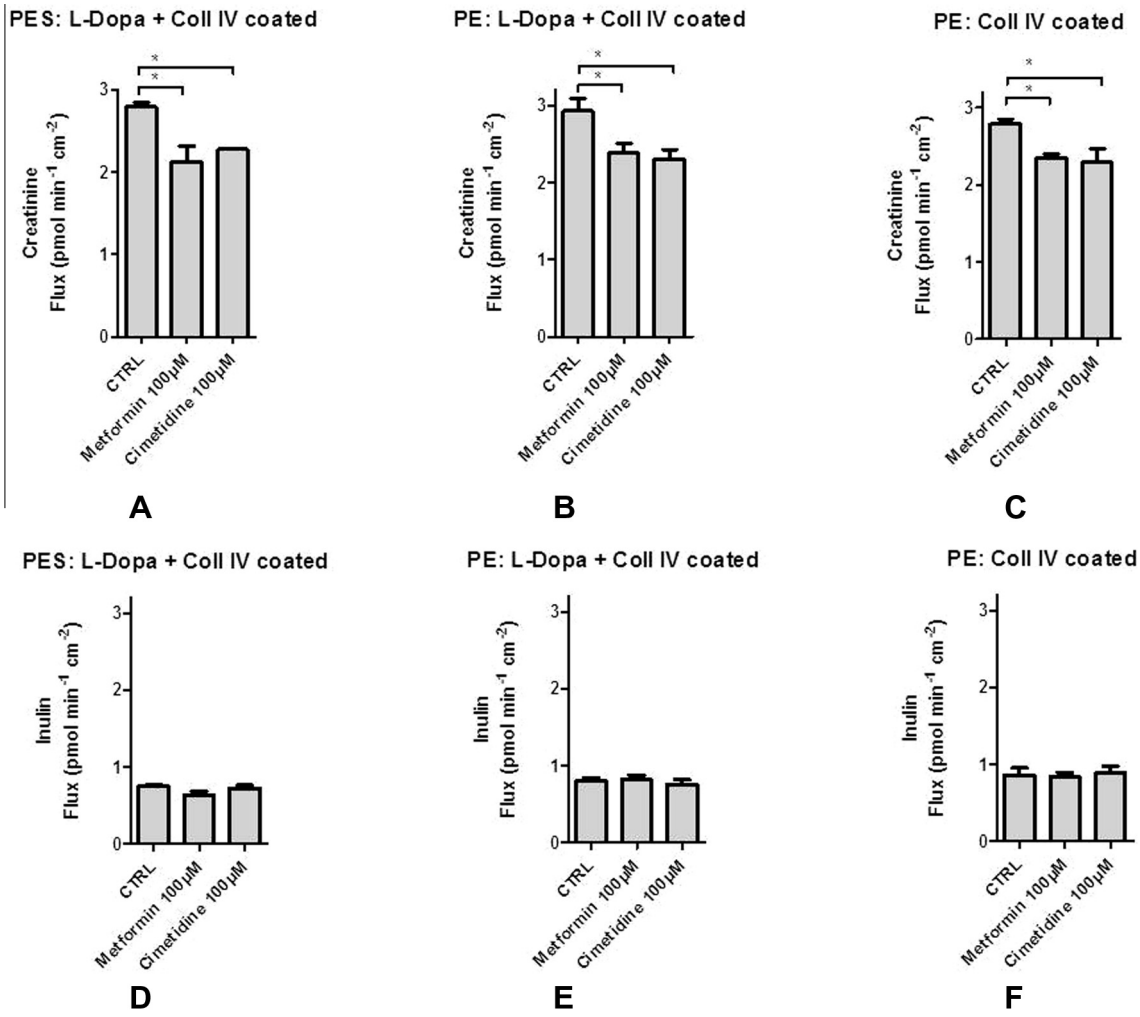

Fig. 6. Basolateral to apical fluxes of (a–c) [^{14}C]creatinine (0.75 μM) and (d–f) [^{3}H]inulin (0.45 μM) across ciPTEC monolayers. Measurements were performed in the presence or absence of the inhibitors metformin (100 μM) or cimetidine (100 μM). Depicted are ciPTEC monolayers cultured on: (a, d) PES-50 Transwell® inserts coated with L-DOPA (1 h) and Coll IV; (b, e) polyester Transwell® membranes coated with L-DOPA (1 h) and Coll IV; (c, f) polyester Transwell® membranes coated with Coll IV only. All coatings were applied for 4 min at the following concentration: L-DOPA 2 mg ml^{-1}, Coll IV 25 mg ml^{-1}. Data are presented as mean ± standard error, $N = 3$. *$p < 0.05$.

tively, ~96% lower than the water permeance through the same membranes ($p < 0.05$). There was no significant difference in protein solution permeance for the coated membranes, as values ranged from 37 ± 27 l m^{-2} h^{-1} bar^{-1} to 65 ± 24 l m^{-2} h^{-1} bar^{-1}. Both BSA (66 kDa) and IgG (150 kDa) were almost completely rejected by both uncoated and coated membranes: the SC <0.1, consistent with what is expected for a 50 kDa membrane.

Given the similarity between the transport properties and the similar cell behavior for the membranes with the optimized coatings, the transport of inulin and creatinine was measured on membranes coated with the coating which required the shortest experimental time: L-DOPA (1 h) with a coating time of 4 min for both L-DOPA and Coll IV (Fig. 1, XII). Transepithelial transport of [^{14}C]creatinine was measured in the presence and absence of transporter substrates, acting as competitors to inhibit uptake. In the kidney, ~20% of creatinine is actively transported by organic cation transport proteins [44]. The functionality of the basolateral cation uptake by OCTs in ciPTEC has previously been demonstrated [7]. Here, Fig. 6 presents the transmembrane flux of [^{14}C]creatinine (0.75 μM, Fig. 6a–c) and [^{3}H]inulin (0.45 μM, Fig. 6d–f) by ciPTEC cell monolayers, cultured on double-coated PES-50, polyester Transwell® membranes or Coll IV coated polyester Transwell® membranes. The paracellular leakage of [^{3}H]inulin across the monolayer was used as an indicator of passive diffusion and hence monolayer tightness, since active transcellular transport has not been reported for this compound [45]. In all cases, the inulin leakage was very low, indicating that a tight monolayer was achieved. The observed average leakage of 0.8 ± 0.1 pmol min^{-1} cm^{-2} (0.1% of the total inulin amount) is comparable to observations made in previous studies that utilized MDCK or LCC-PK cells [46]. In accordance, the organic cation transport inhibitors, metformin and cimetidine, did not affect inulin transport across the cell monolayers. The creatinine flux through the double-coated "living" PES-50 membranes (2.8 ± 0.1 pmol min^{-1} cm^{-2}) was 3.5 times higher than the inulin flux (0.8 ± 0.03 pmol min^{-1} cm^{-2}). Importantly, the creatinine flux was significantly decreased by the inhibitors metformin (24 ± 6% decrease, $p < 0.05$) and cimetidine (18 ± 0.2% decrease, $p < 0.05$), indicating that the developed living membrane actively secretes creatinine. The results of the living PES-50 membranes were comparable to those obtained for cells cultured on the golden standard polyester–Coll IV Transwell® system (see Fig. 6 and Fig. A.3 in the appendix, which compare the permeance of inulin and creatinine through the various membranes).

Various studies have used cellular over-expression models to demonstrate transepithelial creatinine transport. We currently show this transepithelial secretory pathway is endogenously present and functional in ciPTEC. Limited data are available for creatinine fluxes in human renal cells. Brown et al. reported transepithelial creatinine fluxes for primary human proximal tubule epithelial cells [47]. Although we observed lower creatinine fluxes in ciPTEC, the transport capacity is maintained for up to 40 passages (unpublished data). This underscores the robustness of this model and its potential application in a RAD. The use of an immortal cell line provides unlimited proliferative capacity, providing the option to expand the surface area of the living membrane necessary to reach the required clearance levels.

Previous studies have shown that the proximal tubule cell can take up free L-DOPA through the OCT system, thereby influencing cellular processes [48,49]. However, since the L-DOPA coating was fully polymerized before application of Coll IV, and several additional pre-culture washing steps had been applied, no free L-DOPA is expected to be present when culturing the cells. This is supported by the finding that no detrimental effect of the coating was observed for either transepithelial ^{14}C-creatinine transport or the morphology of ciPTEC.

Although we focused here on creatinine transport as a marker for endogenous secretion processes in ciPTEC, creatinine is not the only substance that has to be cleared from the blood. Many cationic and anionic waste products, including indoxyl sulfate, hippuric acid, kynurenic acid, polyamines and guanidines, are retained in patients suffering from uremia [50]. Previously, we reported that ciPTECs functionally express various membrane transport proteins that are involved in the uptake and excretion of uremic toxins [7,30,51]. Therefore a device based on cultured monolayers of ciPTECs grown on modified PES-50 surfaces could provide the ideal tool in the removal of these compounds. The use of sophisticated bioanalysis techniques such as LC-MS/MS might provide more opportunities for the transepithelial transport measurements of these toxic compounds by ciPTEC monolayers [52]. As a next step in RAD development, long term stability and preservation of functionality in ciPTEC monolayers should be evaluated. Even though disruption of the ciPTEC monolayer would be unexpected due to its suppressed proliferation at 37 °C, systematic investigation is required. Furthermore, the introduction of dynamic culture conditions could improve both the formation of tight junctions and cellular transport properties [53]. Recent work suggests beneficial effects of shear stress on renal epithelia, leading to increased endocytosis [46] and sodium reabsorption by the NHE3 receptor [54,55]. Evaluation of the shear stress on the functionality of a transporting ciPTEC monolayer would provide valuable information for RAD development.

4. Conclusions and outlook

In this study, we showed the proof of concept for creating a living membrane by combining functional ciPTEC with PES-50 membranes coated with L-DOPA and Coll IV. The coating was optimized to achieve retention of vital blood components whilst preserving high water permeance and optimal cell monolayer formation. The transport of creatinine through the developed living membrane was comparable to golden standard systems for studying transepithelial transport across proximal tubule monolayers in vitro. The results reported here are promising for the development of a bioartificial kidney. Further investigations are required to establish the long-term stability of these functional renal cell monolayers; the results reported here are promising for the development of a RAD. Future studies will be directed towards producing living membranes on hollow fiber PES-based membranes and to evaluate up-scaling in a bioreactor system to develop a clinically relevant device.

Conflict of interest

The authors declare no conflicts of interest.

Acknowledgments

This research forms part of the Project P3.01 BioKid of the research program of the BioMedical Materials institute, co-funded by the Dutch Ministry of Economic Affairs. The financial contribution of the Dutch Kidney Foundation is gratefully acknowledged.

Appendix A

The effect of two different L-DOPA and Coll IV concentrations on cell adhesion (by using optimized coating with 3 h L-DOPA dissolution and 1 min coating for both L-DOPA and Coll IV) was tested. Uniformity was evaluated upon visual inspection with confocal microscopy, for which two representative membrane areas of each sample were analyzed (see Fig. A.2). The most uniform monolayer on the complete membrane surface was obtained when a double coating of 2 mg ml^{-1} L-DOPA and 25 μg ml^{-1} Coll IV was applied (Fig. A.2c). Thus, no differences in coating concentration were introduced by the optimization performed with respect to previously published data [10].

The basolateral to apical inulin diffusion and creatinine apparent permeability (P_{app}) were calculated with the following equation:

$$P_{app} = \frac{J}{C_b - C_a}$$

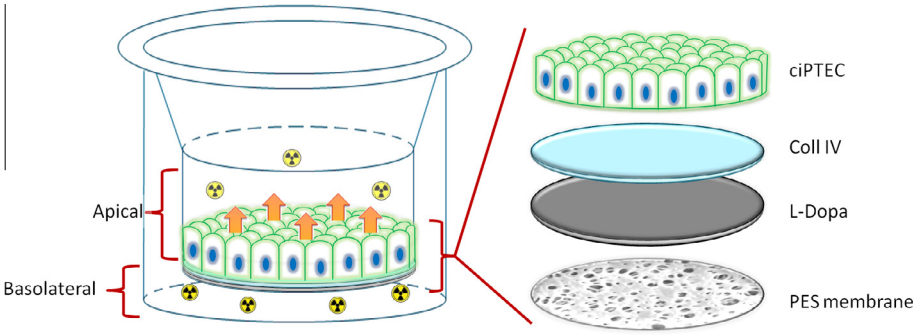

Fig. A.1. Schematic overview of the Transwell® set-up, as used for the examination of basolateral to apical creatinine and inulin transmembrane transport across ciPTEC monolayers. Indicated on the left are the basolateral and apical compartments. On the right side the ciPTEC monolayer and the L-DOPA Coll-IV double coating have been schematically represented.

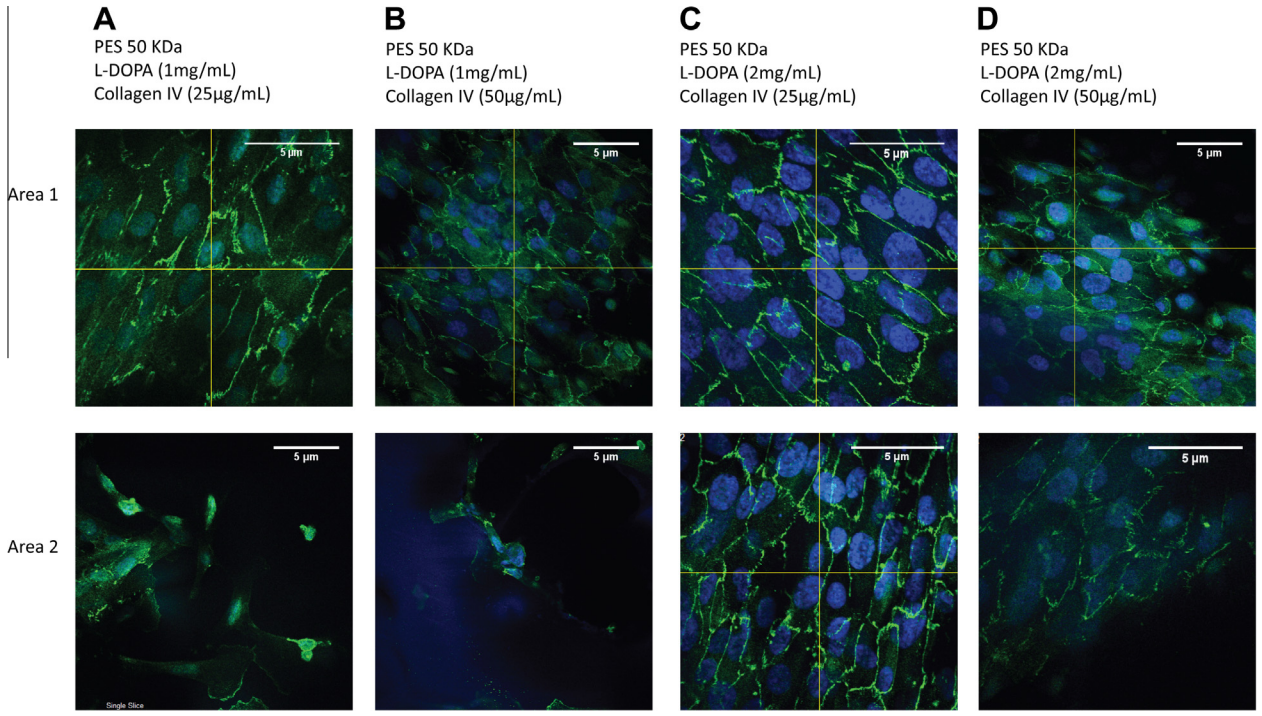

Fig. A.2. Immunocytochemical analysis of the ZO-1 tight junction protein (green) and nuclei (blue) in ciPTEC monolayers cultured on polyester or PES Transwell® inserts coated by 4 min contact to L-DOPA (1 h) and Coll IV using varying coating concentrations: (a) L-DOPA (1 mg ml^{-1}) and Coll IV (25 µg ml^{-1}); (b) L-DOPA (1 mg ml^{-1}) and Coll IV (50 µg ml^{-1}); (c) L-DOPA (2 mg ml^{-1}) and Coll IV (25 µg ml^{-1}); (d) L-DOPA (2 mg ml^{-1}) and Coll IV (50 µg ml^{-1}). Magnification 60× (with an additional 1.4× magnification in A1, C1 and 2, and D2). At least three independent membranes were examined for each condition.

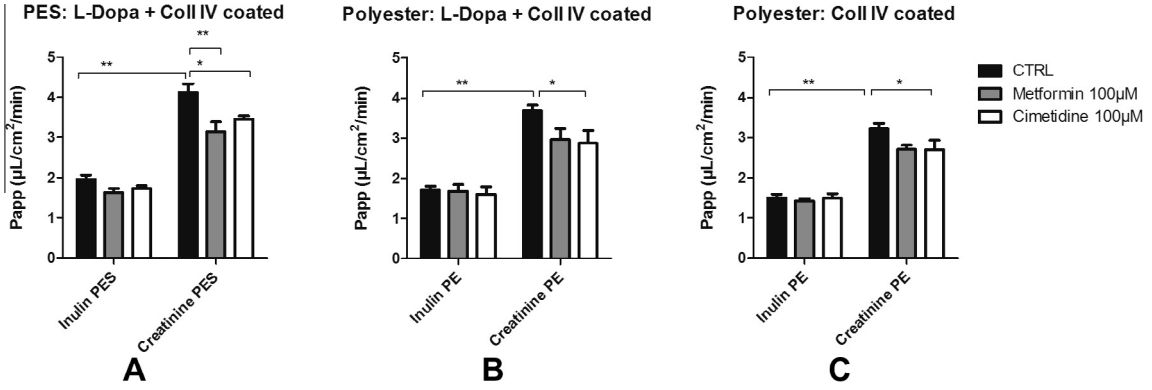

Fig. A.3. Basolateral to apical [^{14}C]creatinine (0.75 µM) and (d–f) [^{3}H]inulin (0.45 µM) transmembrane transport across ciPTEC monolayers. Measurements were performed in the presence or absence of the inhibitors metformin (100 µM) or cimetidine (100 µM). Apparent permeability levels were measured for monolayers cultured on (a) PES-50 Transwell® inserts coated with L-DOPA (1 h) and Coll IV, (b) polyester (PE) Transwell® membranes coated with L-DOPA (1 h) (2 mg ml^{-1}) and Coll IV (25 µg ml^{-1}), (c) polyester Transwell® membranes coated with Coll IV only. All coatings were applied for 4 min at the following concentration: L-DOPA 2 mg ml^{-1}, Coll IV 25 mg ml^{-1}. Data are presented as mean ± standard error, $N = 3$. $^{*}p < 0.05$, $^{**}p < 0.005$, $^{***}p < 0.001$.

where J is the flux, C_b is the initial concentration in the basolateral compartment and C_a is the initial concentration in the apical compartment. For the double-coated PES-50 and polyester membranes the transepithelial transport levels were 2.2 ± 0.4 and 1.97 ± 0.3 µl cm^{-2} min^{-1}, respectively. For the standard polyester Transwells® coated with Coll IV this value was 1.8 ± 0.3 µl cm^{-2} min^{-1}.

Appendix B. Figures with essential color discrimination

Certain figures in this article, particularly Figs. 4 and 5 are difficult to interpret in black and white. The full color images can be found in the on-line version, at http://dx.doi.org/10.1016/j.actbio.2014.12.002.

References

[1] USRDS. 2014 Annual Data Report: epidemiology of kidney disease in the United States. Bethesda, MD: National Institutes of Health, National Institute of Diabetes and Digestive and Kidney Diseases; 2014.
[2] Wolfe RA, Ashby VB, Milford EL, Ojo AO, Ettenger RE, Agodoa LY, et al. Comparison of mortality in all patients on dialysis, patients on dialysis awaiting transplantation, and recipients of a first cadaveric transplant. N Engl J Med 1999;341:1725–30.
[3] Vanholder R, De Smet R, Glorieux G, Argiles A, Baurmeister U, Brunet P, et al. Review on uremic toxins: classification, concentration, and interindividual variability. Kidney Int 2003;63:1934–43.
[4] Meyer TW, Walther JL, Pagtalunan ME, Martinez AW, Torkamani A, Fong PD, et al. The clearance of protein-bound solutes by hemofiltration and hemodiafiltration. Kidney Int 2005;68:867–77.
[5] Krieter DH, Hackl A, Rodriguez A, Chenine L, Moragues HL, Lemke HD, et al. Protein-bound uraemic toxin removal in haemodialysis and post-dilution haemodiafiltration. Nephrol Dial Transplant 2010;25:212–8.

[6] El-Sheikh AA, Masereeuw R, Russel FG. Mechanisms of renal anionic drug transport. Eur J Pharmacol 2008;585:245–55.
[7] Schophuizen CM, Wilmer MJ, Jansen J, Gustavsson L, Hilgendorf C, Hoenderop JG, et al. Cationic uremic toxins affect human renal proximal tubule cell functioning through interaction with the organic cation transporter. Pflugers Arch 2013;465:1701–14.
[8] Humes HD, Buffington D, Westover AJ, Roy S, Fissell WH. The bioartificial kidney: current status and future promise. Pediatr Nephrol 2014;29:343–51.
[9] Jansen J, Fedecostante M, Wilmer MJ, van den Heuvel LP, Hoenderop JG, Masereeuw R. Biotechnological challenges of bioartificial kidney engineering. Biotechnol Adv 2014;32:1317–27.
[10] Oo ZY, Deng R, Hu M, Ni M, Kandasamy K, bin Ibrahim MS, et al. The performance of primary human renal cells in hollow fiber bioreactors for bioartificial kidneys. Biomaterials 2011;32:8806–15.
[11] Fey-Lamprecht F, Gross U, Groth TH, Albrecht W, Paul D, Fromm M, et al. Functionality of MDCK kidney tubular cells on flat polymer membranes for biohybrid kidney. J Mater Sci Mater Med 1998;9:711–5.
[12] Fey-Lamprecht F, Groth T, Albrecht W, Paul D, Gross U. Development of membranes for the cultivation of kidney epithelial cells. Biomaterials 2000;21:183–92.
[13] Sato Y, Terashima M, Kagiwada N, Tun T, Inagaki M, Kakuta T, et al. Evaluation of proliferation and functional differentiation of LLC-PK1 cells on porous polymer membranes for the development of a bioartificial renal tubule device. Tissue Eng 2005;11:1506–15.
[14] Kanai N, Fujita Y, Kakuta T, Saito A. The effects of various extracellular matrices on renal cell attachment to polymer surfaces during the development of bioartificial renal tubules. Artif Organs 1999;23:114–8.
[15] Zhang H, Tasnim F, Ying JY, Zink D. The impact of extracellular matrix coatings on the performance of human renal cells applied in bioartificial kidneys. Biomaterials 2009;30:2899–911.
[16] Fujita Y, Kakuta T, Asano M, Itoh J, Sakabe K, Tokimasa T, et al. Evaluation of Na^+ active transport and morphological changes for bioartificial renal tubule cell device using Madin-Darby canine kidney cells. Tissue Eng 2002;8:13–24.
[17] Ip TK, Aebischer P, Galletti PM. Cellular control of membrane permeability. Implications for a bioartificial renal tubule. ASAIO Trans 1988;34:351–5.
[18] van der Aa MA, Helmerhorst TJ, Siesling S, Riemersma S, Coebergh JW. Vaginal and (uncommon) cervical cancers in the Netherlands, 1989–2003. Int J Gynecol Cancer 2010;20:638–45.
[19] Oliver JA, Barasch J, Yang J, Herzlinger D, Al-Awqati Q. Metanephric mesenchyme contains embryonic renal stem cells. Am J Physiol Renal Physiol 2002;283:F799–809.
[20] Lee H, Rho J, Messersmith PB. Facile conjugation of biomolecules onto surfaces via mussel adhesive protein inspired coatings. Adv Mater 2009;21:431–4.
[21] Lee H, Dellatore SM, Miller WM, Messersmith PB. Mussel-inspired surface chemistry for multifunctional coatings. Science 2007;318:426–30.
[22] Humes HD, MacKay SM, Funke AJ, Buffington DA. Tissue engineering of a bioartificial renal tubule assist device: in vitro transport and metabolic characteristics. Kidney Int 1999;55:2502–14.
[23] Fissell WH, Lou L, Abrishami S, Buffington DA, Humes HD. Bioartificial kidney ameliorates gram-negative bacteria-induced septic shock in uremic animals. J Am Soc Nephrol 2003;14:454–61.
[24] Inagaki M, Yokoyama TA, Sawada K, Duc VM, Kanai G, Lu J, et al. Prevention of LLC-PK(1) cell overgrowth in a bioartificial renal tubule device using a MEK inhibitor, U0126. J Biotechnol 2007;132:57–64.
[25] Terashima M, Fujita Y, Sugano K, Asano M, Kagiwada N, Sheng Y, et al. Evaluation of water and electrolyte transport of tubular epithelial cells under osmotic and hydraulic pressure for development of bioartificial tubules. Artif Organs 2001;25:209–12.
[26] Shitara Y, Horie T, Sugiyama Y. Transporters as a determinant of drug clearance and tissue distribution. Eur J Pharm Sci 2006;27:425–46.
[27] Tahara H, Kusuhara H, Endou H, Koepsell H, Imaoka T, Fuse E, et al. A species difference in the transport activities of H2 receptor antagonists by rat and human renal organic anion and cation transporters. J Pharmacol Exp Ther 2005;315:337–45.
[28] Fissell WH, Manley S, Westover A, Humes HD, Fleischman AJ, Roy S. Differentiated growth of human renal tubule cells on thin-film and nanostructured materials. ASAIO J 2006;52:221–7.
[29] Humes HD, Weitzel WF, Bartlett RH, Swaniker FC, Paganini EP, Luderer JR, et al. Initial clinical results of the bioartificial kidney containing human cells in ICU patients with acute renal failure. Kidney Int 2004;66:1578–88.
[30] Wilmer MJ, Saleem MA, Masereeuw R, Ni L, Van Der Velden TJ, Russel FG, et al. Novel conditionally immortalized human proximal tubule cell line expressing functional influx and efflux transporters. Cell Tissue Res 2010;339:449–57.
[31] Jansen J, Schophuizen CM, Wilmer MJ, Lahham SH, Mutsaers HA, Wetzels JF, et al. A morphological and functional comparison of proximal tubule cell lines established from human urine and kidney tissue. Exp Cell Res 2014;323:87–99.
[32] Wilmer MJ, Saleem MA, Masereeuw R, Ni L, van der Velden TJ, Russel FG, et al. Novel conditionally immortalized human proximal tubule cell line expressing functional influx and efflux transporters. Cell Tissue Res 2010;339:449–57.
[33] Tijink M, Janssen J, Timmer M, Austen J, Aldenhoff Y, Kooman J, et al. Development of novel membranes for blood purification therapies based on copolymers of N-vinylpyrrolidone and n-butylmethacrylate. J Mater Chem B 2013;1:6066–77.
[34] Sweet DH, Miller DS, Pritchard JB. Basolateral localization of organic cation transporter 2 in intact renal proximal tubules. Am J Physiol Renal Physiol 2000;279:F826–34.
[35] Green D, Perry R. Perry's chemical engineers' handbook. 8th ed. New York: McGraw-Hill Education; 2007.
[36] Schneider CA, Rasband WS, Eliceiri KW. NIH Image to ImageJ: 25 years of image analysis. Nat Methods 2012;9:671–5.
[37] Kokko JP, Burg MB, Orloff J. Characteristics of NaCl and water transport in the renal proximal tubule. J Clin Invest 1971;50:69–76.
[38] Azari S, Zou L. Using zwitterionic amino acid L-DOPA to modify the surface of thin film composite polyamide reverse osmosis membranes to increase their fouling resistance. J Membr Sci 2012;401–402:68–75.
[39] Azari S, Zou L, Cornelissen E, Mukai Y. Facile fouling resistant surface modification of microfiltration cellulose acetate membranes by using amino acid L-DOPA. Water Sci Technol 2013;68:901–8.
[40] Cheng C, Li S, Zhao W, Wei Q, Nie S, Sun S, et al. The hydrodynamic permeability and surface property of polyethersulfone ultrafiltration membranes with mussel-inspired polydopamine coatings. J Membr Sci 2012;417–418:228–36.
[41] McCloskey BD, Park HB, Ju H, Rowe BW, Miller DJ, Chun BJ, et al. Influence of polydopamine deposition conditions on pure water flux and foulant adhesion resistance of reverse osmosis, ultrafiltration, and microfiltration membranes. Polymer 2010;51:3472–85.
[42] Bernsmann F, Ponche A, Ringwald C, Hemmerle J, Raya J, Bechinger B, et al. Characterization of dopamine–melanin growth on silicon oxide. J Phys Chem C 2009;113:8234–42.
[43] Ito K, Suzuki H, Horie T, Sugiyama Y. Apical/basolateral surface expression of drug transporters and its role in vectorial drug transport. Pharm Res 2005;22:1559–77.
[44] Ciarimboli G, Lancaster CS, Schlatter E, Franke RM, Sprowl JA, Pavenstadt H, et al. Proximal tubular secretion of creatinine by organic cation transporter OCT2 in cancer patients. Clin Cancer Res 2012;18:1101–8.
[45] Perrone RD. Means of clinical evaluation of renal disease progression. Kidney Int Suppl 1992;36:S26–32.
[46] Raghavan V, Rbaibi Y, Pastor-Soler NM, Carattino MD, Weisz OA. Shear stress-dependent regulation of apical endocytosis in renal proximal tubule cells mediated by primary cilia. Proc Natl Acad Sci U S A 2014;111:8506–11.
[47] Brown CD, Sayer R, Windass AS, Haslam IS, De Broe ME, D'Haese PC, et al. Characterisation of human tubular cell monolayers as a model of proximal tubular xenobiotic handling. Toxicol Appl Pharmacol 2008;233:428–38.
[48] Grundemann D, Koster S, Kiefer N, Breidert T, Engelhardt M, Spitzenberger F, et al. Transport of monoamine transmitters by the organic cation transporter type 2, OCT2. J Biol Chem 1998;273:30915–20.
[49] Pinto-do OP, Soares-da-Silva P. Studies on the pharmacology of the inward transport of L-DOPA in rat renal tubules. Br J Pharmacol 1996;118:741–7.
[50] Duranton F, Cohen G, De Smet R, Rodriguez M, Jankowski J, Vanholder R, et al. Normal and pathologic concentrations of uremic toxins. J Am Soc Nephrol 2012;23:1258–70.
[51] Mutsaers HA, Wilmer MJ, van den Heuvel LP, Hoenderop JG, Masereeuw R. Basolateral transport of the uraemic toxin p-cresyl sulfate: role for organic anion transporters? Nephrol Dial Transplant 2011;26:4149.
[52] Mutsaers HA, Engelke UF, Wilmer MJ, Wetzels JF, Wevers RA, van den Heuvel LP, et al. Optimized metabolomic approach to identify uremic solutes in plasma of stage 3–4 chronic kidney disease patients. PLoS ONE 2013; 8:e71199.
[53] Weinbaum S, Duan Y, Satlin LM, Wang T, Weinstein AM. Mechanotransduction in the renal tubule. Am J Physiol Renal Physiol 2010;299:F1220–36.
[54] McDonough AA. Mechanisms of proximal tubule sodium transport regulation that link extracellular fluid volume and blood pressure. Am J Physiol Regul Integr Comp Physiol 2010;298:R851–61.
[55] Wang T. Flow-activated transport events along the nephron. Curr Opin Nephrol Hypertens 2006;15:530–6.